BBA - General Subjects 1865 (2021) 129897

Contents lists available at ScienceDirect

BBA - General Subjects

journal homepage: www.elsevier.com/locate/bbagen

Efficient photodynamic inactivation of *Leishmania* parasites mediated by lipophilic water-soluble Zn(II) porphyrin ZnTnHex-2-PyP^{4+}

Tiago H.S. Souza [a,e], Camila G. Andrade [a], Fernanda V. Cabral [b], José F. Sarmento-Neto [c], Júlio S. Rebouças [c], Beate S. Santos [d], Martha S. Ribeiro [b], Regina C.B.Q. Figueiredo [e,1], Adriana Fontes [a,*,1]

[a] Departamento de Biofísica e Radiobiologia, Universidade Federal de Pernambuco, Recife, PE, Brazil
[b] Centro de Lasers e Aplicações, Instituto de Pesquisas Energéticas e Nucleares (IPEN-CNEN/SP), São Paulo, SP, Brazil
[c] Departamento de Química, Universidade Federal da Paraíba, João Pessoa, PB, Brazil
[d] Departamento de Ciências Farmacêuticas, Universidade Federal de Pernambuco, Recife, PE, Brazil
[e] Departamento de Microbiologia, Instituto Aggeu Magalhães- Fundação Oswaldo Cruz, Recife, PE, Brazil

ARTICLE INFO

Keywords:
Antimicrobial photodynamic therapy
Blue LED
Leishmania amazonensis
Leishmania braziliensis
Photodynamic therapy
ZnTnHex-2-PyP^{4+}

ABSTRACT

Background: Photodynamic inactivation (PDI) is emerging as a promising alternative for cutaneous leishmaniasis (CL). The chemotherapy currently used presents adverse effects and cases of drug resistance have been reported. ZnTnHex-2-PyP^{4+} is a porphyrin with a high potential as a photosensitizer (PS) for PDI, due to its photophysical properties, structural stability, and cationic/amphiphilic character that can enhance interaction with cells. This study aimed to investigate the photodynamic effects mediated by ZnTnHex-2-PyP^{4+} on *Leishmania* parasites.
Methods: ZnTnHex-2-PyP^{4+} stability was evaluated using accelerated solvolysis conditions. The photodynamic action on promastigotes was assessed by (i) viability assays, (ii) mitochondrial membrane potential evaluation, and (iii) morphological analysis. The PS-promastigote interaction was studied. PDI on amastigotes and the cytotoxicity on macrophages were also analyzed.
Results: ZnTnHex-2-PyP^{4+}, under submicromolar concentration, led to immediate inactivation of more than 95% of promastigotes. PDI promoted intense mitochondrial depolarization, loss of the fusiform shape, and plasma membrane wrinkling in promastigotes. Fluorescence microscopy revealed a punctate PS labeling in the parasite cytoplasm. PDI also led to reductions of *ca.* 64% in the number of amastigotes/macrophage and 70% in the infection index after a single treatment session. No noteworthy toxicity was observed on mammalian cells.
Conclusions: ZnTnHex-2-PyP^{4+} is stable against demetallation and more efficient as PS than the ethyl analogue ZnTE-2-PyP^{4+}, indicating readiness for evaluation in *in vivo* studies as an alternative approach to CL.
General significance: This report highlighted promising photodynamic effects mediated by ZnTnHex-2-PyP^{4+} on *Leishmania* parasites, opening up perspectives for applications in CL pre-clinical assays and PDI of other microorganisms.

1. Introduction

Leishmaniasis, a disease caused by a parasite of the genus *Leishmania*, is considered one of the most common neglected parasitic diseases in the world, with more than 12 million people infected [1]. Cutaneous leishmaniasis (CL) is the most common form of this disease, transmitted to mammalian hosts by infected female phlebotomine sandflies. CL is usually caused by *L. braziliensis*, *L. amazonensis*, and *L. guyanensis* in the New World (American continent). The parasite life cycle involves two distinct forms: the promastigote – found in the phlebotomine sandfly vector – and the intracellular amastigote – found in host mammalian cells. The cycle can restart during blood meal by sandflies in an infected host [1,2].

Currently, the drugs of choice to treat CL, such as pentavalent antimonials, amphotericin B, and pentamidine are administrated systemically, have high toxicity and present adverse effects, which often limit

* Corresponding author at: Departamento de Biofísica e Radiobiologia, Universidade Federal de Pernambuco, Recife, PE, Brazil.
E-mail address: adriana.fontes@ufpe.br (A. Fontes).
[1] These authors jointly supervised this work.

https://doi.org/10.1016/j.bbagen.2021.129897
Received 13 January 2021; Received in revised form 29 March 2021; Accepted 29 March 2021
Available online 1 April 2021

their use. In addition, cases of parasite resistance to conventional treatments have been reported [3,4]. Photodynamic therapy (PDT) has emerged as an alternative modality to treat CL [4,5]. PDT has been widely studied not only for use in cancer treatments, but also as a promising option to induce the death of microorganisms, for which the term photodynamic inactivation (PDI) is often used. Among other advantages, PDT is expected to provide a fast and localized treatment [6].

PDT/PDI is based on the use of substances with photosensitizing properties, followed by their photoactivation in the presence of oxygen. After light irradiation, the activation of the photosensitizer (PS) results in the generation of reactive oxygen species (ROS) that lead to death of the target cell by oxidative stress. The potential of PDT lies in the combination of (i) a local treatment, (ii) the PS intracellular location since the ROS action is limited to the PS accumulation site, due to ROS lifetime, and (iii) a more effective and complete antioxidant system of healthy mammalian cells than the protozoan cells, for example. The use of PDT over standard therapy for CL can also include the advantage of being minimally invasive. It should be noted that since the ROS effect can reach several subcellular targets, cases reporting on parasite resistance have not yet been found [6–8].

The use of different PSs, such as curcumin and methylene blue, combined with varied irradiation parameters for the inactivation of *Leishmania* parasites have been reported in the literature [9,10]. Thus, the importance of the search for alternative PSs that may be efficient under lower concentrations, with shorter pre-incubation times, and mild irradiation conditions, reducing the photodamage to adjacent tissues. A better understanding of the interaction of the different PSs with the biological target is important to optimize protocols and procedures.

Porphyrins and their metal-containing derivatives are tetrapyrrole compounds that have already been evaluated as PSs in various studies, especially related to the annihilation of cancer cells [11]. Porphyrins present interesting features and advantages for PDT, such as (i) optimized photophysical properties suitable for photodynamic processes; (ii) structural versatility for tailored lipophilicity and ionic character, facilitating and modulating both bioavailability and interaction with cellular structures; and (iii) high efficiency intracellular ROS generation. Moreover, metalloporphyrin complexes with Zn(II) have the potential to be even more effective PSs than their free-base analogs. The chelation of Zn(II) in the structure of porphyrins increases the chemical stability, enhances their interaction with cell membranes, and promotes a long triplet lifetime leading to a higher singlet oxygen quantum yield [12–14].

Zn(II) porphyrins have been explored as PSs for their antimicrobial photoinactivation of fungi, bacteria, and also protozoa [15–17]. In bacterial cultures, multiple photodynamic exposures and regrowth of surviving cells or continuous growth under sublethal photodynamic conditions, using Zn(II) porphyrins, did not lead to development of resistance to photosensitizers [18].

We have recently reported promising results in PDI of promastigotes and amastigotes of *L. braziliensis* using Zn(II) *meso*-tetrakis(*N*-ethylpyridinium-2-yl)porphyrin (ZnTE-2-PyP^{4+}, ZnP ethyl) [17]. Nevertheless, experiments carried out by Benov et al. [19] with cancer cells have indicated that the derivative Zn(II) *meso*-tetrakis(*N*-n-hexylpyridinium-2-yl)porphyrin (ZnTnHex-2-PyP^{4+}, ZnP hexyl) can potentially be even more successful for PDI [19]. ZnP hexyl is more lipophilic than ZnP ethyl, but it still maintains water-solubility and an amphiphilic character. Whereas the ZnP ethyl tended to accumulate preferentially in lysosomes and/or was found distributed in the cytoplasm, the ZnP hexyl, due to its higher lipophilicity, interacted better with the cancer cells, especially with organelles that are essential for cell survival, such as mitochondria [12,19,20].

Given that (i) the adverse effects associated with the current therapy for CL, (ii) the need for faster and more effective photodynamic protocols using lower irradiation conditions and PS concentrations, (iii) the promising results obtained by us with the ZnP ethyl, and (iv) the potentialities reported for ZnP hexyl, the present study aimed to evaluate the *in vitro* action of ZnTnHex-2-PyP^{4+} in the inactivation of parasites of *Leishmania* species that cause CL.

2. Methodology

2.1. Zn(II) porphyrins

ZnP hexyl and ZnP ethyl were synthesized by alkylation of the precursor Zn(II) *meso*-tetrakis(2-pyridyl)porphyrin, using an adaptation of the method described by Viana et al. [21], presenting spectral and chromatographic characteristics identical to those previously reported [12,20].

The stability of ZnP hexyl and ZnP ethyl against demetallation in solution was evaluated using accelerated solvolysis studies. ZnP solvolysis half-lives ($t_{½}$) under harsh acidic conditions and in simulated digestive fluids were determined. Aqueous hydrochloric acid (1 M), nitric acid (1 M), and phosphoric acid (1 M) solutions were standardized by titrimetry, whereas simulated gastric fluid (SGF; pH 2.6) and simulated intestinal fluid (SIF; pH 7.0) were prepared as non-enzymatic electrolyte solutions as described elsewhere [22]. SGF was made of 6.9 mM KCl, 0.9 mM KH_2PO_4, 25 mM $NaHCO_3$, 47.2 mM NaCl, 0.1 mM $MgCl_2{\cdot}(H_2O)_6$, 0.5 mM $(NH_4)_2CO_3$, and 0.075 mM $CaCl_2{\cdot}(H_2O)_2$, and the final pH was adjusted to 2.6 with 6 M HCl. The SIF was made up from 6.8 mM KCl, 0.8 mM KH_2PO_4, 85 mM $NaHCO_3$, 38.4 mM NaCl, 0.33 mM $MgCl_2{\cdot}(H_2O)_6$, and 0.3 mM $CaCl_2{\cdot}(H_2O)_2$, with the final pH adjusted to 7.0 with 6 M HCl. The assays were carried out at room temperature (approximately 25 °C) using a Shimadzu UV-1800 UV–vis spectrometer, with resolution of 0.5 nm and wavelength range of 300–800 nm. Briefly, a few microliters of a freshly prepared concentrated aqueous stock solution of ZnP (typically 1 mM) were diluted in 3 mL of solvent (1 M aqueous acid, SGF or SIF) in an UV–vis cuvette to yield a working solution of ZnP in the micromolar concentration range. Upon rapid mixing, the ZnP solvolysis was followed spectrophotometrically immediately and over time. The reaction half-life was determined under pseudo-first order conditions [23,24].

Throughout this work, the concentrations of all ZnP stock solutions were determined spectrophotometrically using published molar absorptivity values for ZnP hexyl ($\varepsilon_{427.0\ nm} = 436{,}516\ cm^{-1}\ M^{-1}$) [12] and ZnP ethyl ($\varepsilon_{425.5\ nm} = 288{,}403\ cm^{-1}\ M^{-1}$) [25].

2.2. Parasites

Promastigotes of *L. amazonensis* (MHOM/77BR/LTB0016) were cultivated in Schneider medium (Gibco), supplemented with 10% heat-inactivated fetal bovine serum (FBS - Gibco), 100 U/mL penicillin, and 100 μg/mL streptomycin antibiotic (Gibco). Cells were maintained at 26 °C and used at the beginning of the stationary growth phase. Promastigote forms of *L. braziliensis* (MHOM/BR/1975/M2903) were also cultivated and used following the same protocol applied to *L. amazonensis*.

Intracellular amastigotes of *L. amazonensis* were obtained by infecting murine peritoneal macrophages (PMs) with promastigotes, simulating the parasite infection cycle in mammals. For this, PMs (5×10^5 cells/well) were adhered to 24-well plates containing a round coverslip (13 mm) at the bottom for 24 h, infected with promastigotes at a ratio of 5:1 (promastigotes:macrophages), and kept in RPMI-1640 medium (Sigma-Aldrich), supplemented with 10% heat-inactivated FBS, at 37 °C and 5% CO_2, for 14 h. After this period, the infection was confirmed under light microscopy before the treatment. PMs were obtained from peritoneal exudates cells of healthy female BALB/c mice (6–8 weeks old) and harvested in 5–7 mL of ice-cold RPMI-1640 medium.

2.3. Photodynamic assay on promastigote forms

Photodynamic assays with promastigote forms were performed in 96-well microplates. Two final concentrations of ZnP hexyl, 0.62 (A) and

1.25 μM (B), were used. Two irradiation conditions were also carried out: Light 1 = *ca.* 38.2 mW/cm^2 for 1 min and Light 2 = *ca.* 19.1 mW/cm^2 for 3 min.

Thus, a total of 8 groups were evaluated: (1) **Control** = without any treatment (in the dark); (2) **Light 1** = treatment only with irradiation at *ca.* 2.3 J/cm^2; (3) **Light 2** = treatment only with irradiation at *ca.* 3.4 J/cm^2; (4) **ZnP** = 1.25 μM ZnP (in the dark); (5) **PDT A1** = 0.62 μM ZnP + Light 1; (6) **PDT A2** = 0.62 μM ZnP + Light 2; (7) **PDT B1** = 1.25 μM ZnP + Light 1; and (8) **PDT B2** = 1.25 μM ZnP + Light 2.

The concentrations, pre-incubation time, and irradiation time herein used were initially chosen based on our previous study carried out with ZnP ethyl [17]. The same irradiation configuration was applied. The systems were irradiated from the top to the bottom, without the plastic cover. A LEDbox (Biolambda) at 410 ± 10 nm was used as the light source (emission spectrum in the Supplementary Material – Section A – Fig. S1). For all groups treated with ZnP hexyl, the cells were pre-incubated with the PS for 5 min in the absence of light. For all the experiments, the promastigote suspension (1×10^7 cells/mL) was transferred to the well and incubated with either 1× phosphate-buffered saline (PBS, for "control" and "only Light" groups) or PBS containing ZnP, in a 1:1 volume proportion (a total volume of 200 μL, prepared at the time).

2.4. Trypan blue evaluation

The promastigote survival was evaluated right after treatment using the trypan blue exclusion method. This method is based on the principle that viable cells are impermeable to the dye, while dead cells absorb trypan blue into their cytoplasm due to loss of membrane selectivity, becoming stained [26]. Trypan blue (10 μL) was added to 90 μL of the parasite suspension, for each evaluated condition. After homogenizing and incubating for 5 min, the number of unstained (viable) parasites was counted in a Neubauer chamber under light microscopy. Four independent experiments were performed in duplicate.

2.5. Morphological analysis

To evaluate morphological alterations induced by the photodynamic treatment on promastigotes, scanning electron microscopy (SEM) assays were performed. *L. amazonensis* parasites (1×10^7 cells/mL) from untreated (Control) and treated groups (Light 2, ZnP, PDT A2, and PDT B2) were submitted to the same incubation and irradiation procedures described in Section 2.3. Then, promastigotes were processed according to the protocol reported by Aliança et al. [27] and observed in a JEOL scanning electron microscope (JSM-5600 LV).

2.6. Cell labeling assay by confocal microscopy

Confocal fluorescence microscopy was applied to analyze the interaction and uptake of ZnP hexyl by *L. amazonensis* promastigotes. Parasites (1×10^6 cells/mL) were placed in confocal microscopy chambers (SPL) and incubated with the PS at 5 μM, for 5 or 15 min. This concentration was chosen to guarantee the detection of a high fluorescence signal from ZnP and acquire sharp and clear images. Samples were observed under a ZEISS LSM 700 at 405 nm excitation, and the PS fluorescence was detected in a multispectral mode at porphyrin emission region.

2.7. Flow cytometry

The photodynamic effects related to membrane permeability and mitochondrial membrane potential (ΔΨm) were also evaluated for promastigotes. For this, parasites submitted to the different experimental conditions were labeled with Propidium Iodide (PI, Sigma-Aldrich) or Rhodamine 123 (Rh 123, Sigma-Aldrich), respectively.

For PI assays, cells were rinsed with PBS and incubated with this probe (final concentration of 30 μg/mL) for 15 min. For ΔΨm, parasites were incubated with Rh 123 (final concentration of 10 μg/mL) for 15 min. After incubation, cells were analyzed using an Accuri C6 flow cytometer (Becton Dickinson) at 488 nm excitation for both, and long pass (LP) 670 nm detection for PI and 533/30 nm detection for Rh 123. Changes in membrane permeability were accessed analyzing the labeling percentages while changes in ΔΨm were evaluated through the medians of fluorescence intensity (MFIs).

For each sample, a total of 20,000 events were acquired. All flow cytometry assays were performed at least in duplicate. Hydrogen peroxide (H_2O_2 – 2.5%) was used as the positive control of cell death due to its ability to induce oxidative damage to cells [28].

2.8. Cytotoxicity assay on mammalian cells

Cytotoxicity assays with mammalian cells were also performed, using bone marrow-derived macrophages (BMDMs), following the protocol reported by Cabral et al. [29]. Briefly, female BALB/c mice (6–8 weeks old) were sacrificed and the femoral and tibial marrows were flushed from the bones with RPMI-1640 medium. The cells were re-suspended and cultured in Petri dishes during 7 days in RPMI-1640 medium (15 mM HEPES, 2 g sodium bicarbonate/L, and 1 mM L-glutamine – Gibco), and supplemented with 20% of a colony stimulating factor (L-929) and 20% FBS (Sigma-Aldrich), at 37 °C and 5% CO_2. Posteriorly, BMDMs were centrifuged, counted, and seeded (1×10^5 cells/well) in 96-well plates containing RPMI-1640 medium, supplemented with 10% heat-inactivated FBS, adhered overnight at 37 °C and 5% CO_2. Then, the culture supernatant was removed and ZnP hexyl at concentrations of 0.62 or 1.25 μM was added (except for the "control" and "Light" groups, to which only PBS was added). Treatment at the highest radiant exposure (3.4 J/cm^2) was adopted. The plates were irradiated as previously described for promastigotes and the same pre-incubation time was applied. After treatment, cells were washed and incubated in RPMI-1640 medium containing 5 mg/mL 3-(4,5-dimethylthiazol-2-yl)-2,5-diphenyltetrazolium bromide (MTT, Sigma-Aldrich), at 37 °C and 5% CO_2 for 4 h. After incubation, the supernatant was discarded, and the crystals formed were solubilized in dimethylsulfoxide. Absorbances were measured in a Spectramax M4 spectrophotometer at 570 nm. Tests were performed in triplicates in three independent experiments.

2.9. Photodynamic assay on intracellular amastigote forms

For experiments with intracellular amastigotes, 500 μL of each system (controls and tests) were added to 24-well plates containing macrophages infected by *L. amazonensis*. The same pre-incubation time used for promastigotes was herein applied. The conditions with the highest radiant exposure (PDT A2 and PDT B2) were chosen to assess the photodynamic effect on amastigotes. After each treatment, cells were stained with panoptic, according to the manufacturer's instructions (Laborclin). The number of intracellular amastigotes per macrophage and the percentage of infected macrophages were quantified by analyzing 100 macrophages per coverslip chosen randomly under light microscopy. This evaluation was performed in duplicate, in three independent assays, totaling 600 cells analyzed. The infection index was also obtained using the number of amastigotes per macrophage × % Infection, for the control and treated groups. The % Infection was calculated as the number of infected macrophages/ the total number of macrophages × 100.

2.10. Statistical analysis

Statistical differences between groups were evaluated by the paired Student's *t*-test, after analyzing the normal distribution of the data by Shapiro-Wilk. The software GraphPad Prism version 7.0 was used for data analysis and image creation. Differences were considered

significant when $p < 0.05$.

2.11. Ethical standards

The study involving animals was approved by the "Comitê de Ética em Experimentação Animal – Instituto Aggeu Magalhães/Fundação Oswaldo Cruz" and the "Instituto de Pesquisas Energéticas e Nucleares" (CEUA - FIOCRUZ N° 121/2017; IPEN-CNEN/SP N°. 189/2017). All experiments were carried out in accordance with relevant guidelines and regulations. Animals from breeding facilities of the "Instituto Aggeu Magalhães" and "Instituto de Pesquisas Energéticas e Nucleares" grew up in micro-isolators, receiving autoclaved water and feed offered *ad libitum*. They were kept in air-conditioned rooms, with an automated system for supply and exhaust air changes, and with automatic lighting control 12 h light/12 h dark.

3. Results and discussion

3.1. Stability of Zn(II) porphyrin

Water-soluble Zn(II) *N*-alkylpyridylporphyrins are promising candidates as PDT photosensitizers [12–20]. In general, Zn(II) porphyrins are usually stable in a solid state, but the knowledge of their specific chemical stability in solution under various conditions is relevant to guide storage and handling protocols, formulation strategies, and administration routes.

Zn(II) metalation of porphyrins has been widely explored in synthetic chemistry as an efficient way to increase the chemical and thermal stability of porphyrin derivatives [30]. A common reaction that may compromise Zn(II) porphyrin stability in aqueous media, however, is Zn(II) demetallation *via* hydrolysis. The stability of Zn(II) chelation by porphyrins depends on intrinsic aspects (such as porphyrin ring substituents, peripheral charges, porphyrin basicity, and steric hindrance) [30,31] and extrinsic factors (such as solvent nature, pH, and ionic strength) [32,33]. Thus, in the present work, the stability of ZnP hexyl against demetallation in solution was evaluated using accelerated solvolysis studies under harsh acidic conditions (HCl, HNO_3, and H_3PO_4) and in simulated digestive fluids (data in the Supplementary Material – Section B – Table S1). Accelerated stability studies have evaluated drug degradation under extreme conditions, to approximate their behavior to real conditions [34]. Given the photoeffects mediated by the shorter-chain analog ZnP ethyl PS on *L. braziliensis* previously reported by Andrade et al. [17], we also carried out stability studies on ZnP ethyl for the sake of completeness and comparison with the ZnP hexyl data reported herein.

The acid-catalyzed Zn(II) solvolysis of Zn(II) porphyrins is largely affected by the nature of the anion [30]. Thus, nitric acid, although of little biological significance *per se*, is useful as a readily available acid with an anion of limited coordination capability. At 1 M HNO_3, the half-lives of ZnP methyl [35] and ZnP ethyl (that differ by only one CH_2 group in the alkyl side chains) are *ca.* 1 day and 5 days respectively, in the μM ZnP concentration range. The profound impact of the alkyl side chain on Zn(II) porphyrin stability was confirmed with ZnP hexyl, which showed no detectable Zn(II) loss after a week [36]. Based on the biological relevance of chloride and phosphate anions in biological media, assays using 1 M HCl or 1 M H_3PO_4 were carried out. At 1 M HCl, which is an acid with a coordinating anion, the half-lives of both ZnP ethyl and ZnP hexyl dropped considerably to *ca.* 1 and 10 h, respectively (Supplementary Material – Section B – Table S1), in agreement with literature data [37]. Conversely, the ZnP stability was remarkably high at 1 M H_3PO_4; for example, the half-life of ZnP ethyl was *ca.* 9 days. Of note, the addition of 1 M NaCl into the 1 M H_3PO_4 system led to a full demetallation of ZnP ethyl within 24 h, which agrees with the HCl data and reveals the negative role that chloride has in the demetallation of these ZnP systems under accelerated degradation conditions at extremely low pH. Chlorides are good coordinating anions that occupy the coordination positions vacated by the protonated porphyrin nitrogen atoms during solvolysis, further reducing the amount of charge separation needed for Zn(II) dissociation [23]. Considering that the mechanism of ZnP hydrolysis and kinetics are well established, the demetallation of both ZnPs in solution for short periods of time should be negligible at nearly neutral pH [23,30,38].

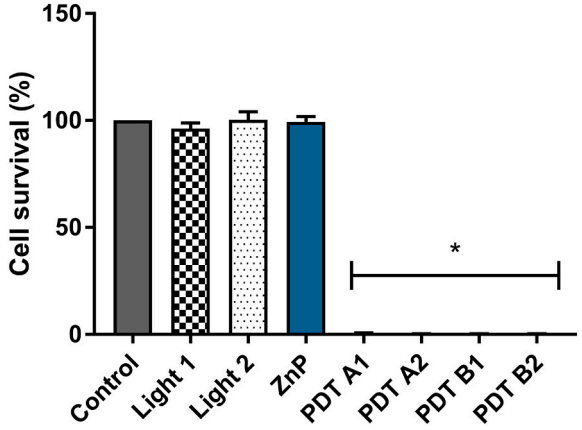

Fig. 1. Survival of *L. amazonensis* promastigotes evaluated by trypan blue assay. **Control –** untreated cells; **Light 1 –** Irradiance 38.2 mW/cm^2 for 1 min (2.3 J/cm^2); **Light 2 –** 19.1 mW/cm^2 irradiance for 3 min (3.4 J/cm^2); **ZnP –** 1.25 μM ZnP hexyl; **PDT A1 –** 0.62 μM ZnP hexyl + Light 1; **PDT A2 –** 0.62 μM ZnP hexyl + Light 2; **PDT B1 –** 1.25 μM ZnP hexyl + Light 1; **PDT B2 –** 1.25 μM ZnP hexyl + Light 2. Data presented as mean ± standard error (SE). *Statistically significant groups ($p < 0.0001$) when compared to control. Four independent experiments were performed in duplicate ($n = 8$).

PDT photosensitizers in general have been used both topically and systemically, *via* injection or oral routes. The application of topical formulation or local injections in CL PDT protocols (as opposed to systemic therapy) is highly desirable and complies well with treatment. Thus, we extended the evaluation of the stability of ZnPs to include conditions that are relevant to a systemic oral administration route. Two standardized simulated digestive fluids were prepared with rich electrolyte composition (K^+, Na^+, Cl^-, $H_2PO_4^-$, HCO_3^-, CO_3^{2-}, Mg^{2+}, NH_4^+, Ca^{2+}) and controlled pH [22]. In both, the simulated gastric fluid (SGF, pH 2.6) and the simulated intestinal fluid (SIF, pH 7.0), no indication of Zn(II) loss was observed for either ZnP hexyl or ZnP ethyl. This suggests that oral administration of either of these ZnPs could be considered in broader *in vivo* situations (those not limited to leishmaniasis) where systemic administration is prescribed or acceptable, such as an alternate/complementary administration route, *e.g.*, for deep lesion treatments [39].

Overall, these data suggest that both cationic ZnPs are stable in solution depending on pH control and concentration of some ions, such as Cl^-. Thus, for short periods (hours-to-days), the preparation of stock solutions and dilutions in distilled water at neutral pH poses no problems regarding ZnP hydrolysis. For longer periods (weeks-to-months), we suggest the use of stocks in phosphate buffers at nearly neutral pH. The use of PBS is unadvised to prevent Cl^--catalyzed hydrolysis, which may become relevant over longer periods (month time-scale). For storage over much longer time periods (months-to-years), we prescribe keeping ZnPs in the solid state.

3.2. Promastigote survival and cell membrane permeability evaluation

The percentage of promastigote survival was evaluated by the trypan blue exclusion method under different conditions. The groups treated only with light or with ZnP hexyl in the dark showed viability results similar to the control (no statistically significant difference observed). Considering both irradiation conditions and ZnP hexyl concentrations (0.62 or 1.25 μM) applied, all photodynamically treated groups

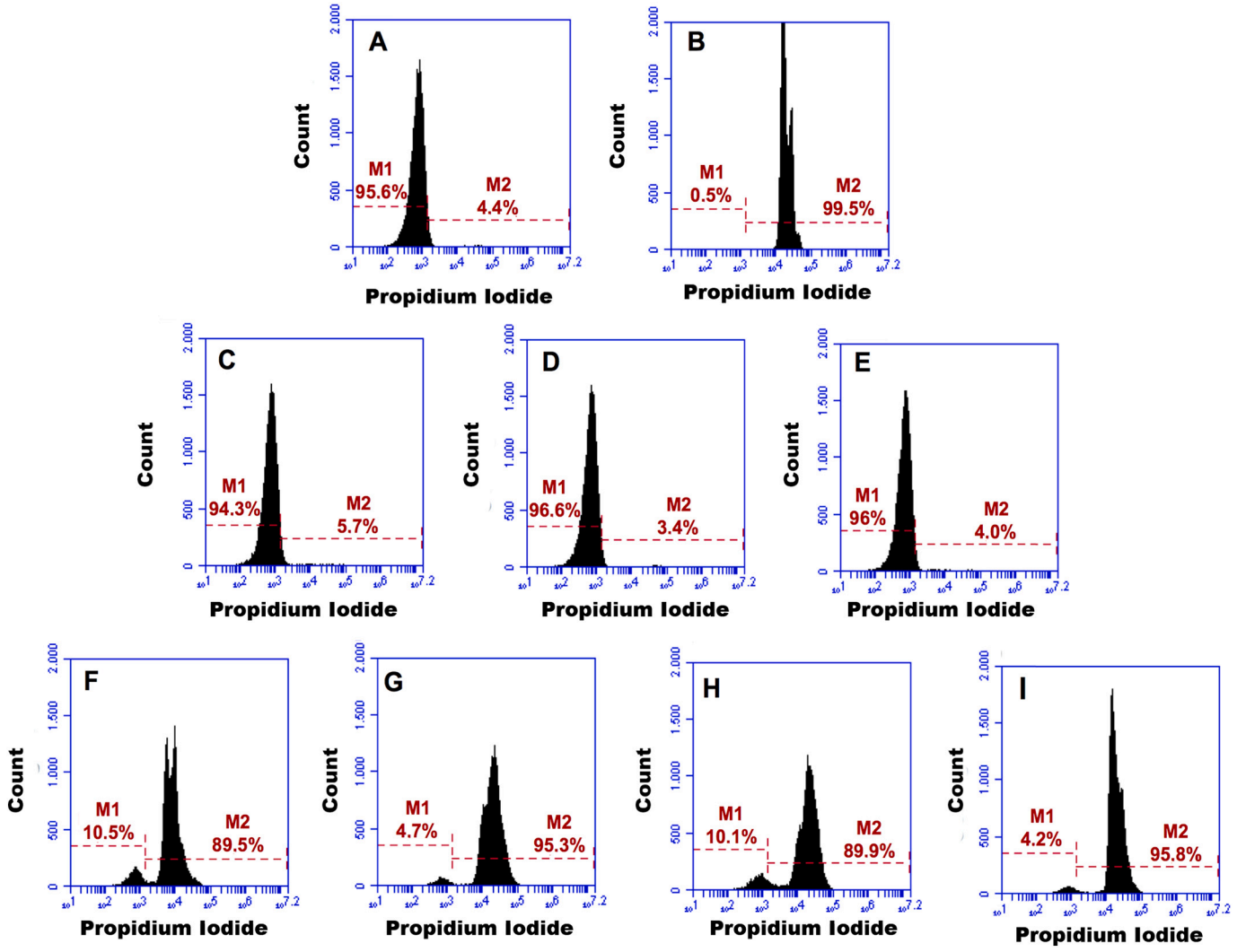

Fig. 2. Representative flow cytometry histograms of *L. amazonensis* promastigotes after incubation with PI. M1 – unlabeled cells; M2 – PI positive labeled cells. **A –** PI (negative control - without treatment); **B –** H_2O_2 (2.5%) – positive control of cell death; **C –** 1.25 μM ZnP hexyl; **D –** Light 1 (2.3 J/cm^2); **E –** Light 2 (3.4 J / cm^2); **F –** 0.62 μM ZnP hexyl + Light 1 (PDT A1); **G –** 0.62 μM ZnP hexyl + Light 2 (PDT A2); **H –** 1.25 μM ZnP hexyl + Light 1 (PDT B1); **I –** 1.25 μM ZnP hexyl + Light 2 (PDT B2). For each sample, a total of 20,000 events were acquired and performed in two independent assays.

exhibited cell death by more than 99% of *L. amazonensis* promastigotes, compared to the control without treatment, as shown in Fig. 1. Thus, incubation with PS, followed by irradiation, had a drastic effect on the parasite viability, indicating an intense decrease in the number of viable cells. ZnP concentrations below 0.62 μM (0.3 and 0.5 μM) were also evaluated; but the percentage of cell death was lower than 90% (data not shown). High percentages of cell death were also observed when *L. braziliensis* promastigotes were submitted to photodynamic treatment (Supplementary Material – Section C – Fig. S2).

A complementary way to assess information on cell survival is by the Propidium Iodide (PI) assay. This dye is an impermeable fluorescent cell membrane probe that binds to cell DNA and RNA when the permeability of plasma membrane is compromised [40]. Fig. 2 illustrates the PI assays evaluated by flow cytometry for *L. amazonensis* promastigote forms submitted or not to photodynamic treatment. Our results showed that only 4.4% of cells from the negative control group (without any treatment) were labeled by PI (Fig. 2A). A similar percentage of labeling was observed for cells treated only with ZnP hexyl (1.25 μM) under the dark condition (Fig. 2C) or treated only with Light 1 or Light 2 (Fig. 2D and E). On the other hand, as expected, 99.5% of cells incubated with the positive control (hydrogen peroxide, H_2O_2 – 2.5%) were PI positive (Fig. 2B), indicating a loss of membrane permeability. Photodynamically treated cells in the presence of ZnP hexyl (Figs. 2F to 2I) also showed intense labeling. Approximately 90% and 96% of cells from PDT groups were positive for PI when Light 1 and Light 2 conditions were, respectively, applied. These effects were independent of the ZnP hexyl concentrations used. The photodynamic effects observed in *L. braziliensis* were similar to those obtained for *L. amazonensis*, as shown in the Supplementary Material – Section D – Fig. S3.

These results corroborate the trypan blue dye assays, indicating that photodynamic treatments led to a considerable increase in cell membrane permeability, causing loss of cell viability.

L. amazonensis and L. braziliensis can exhibit different susceptibilities to drug treatments under the same experimental conditions [41], even when submitted to photodynamic treatment mediated by Zn(II) phthalocyanines [42]. Nevertheless, in this study, these differences were not observed, suggesting an advantage of our approach to the treatment of CL.

Exploring metalloporphyrin-mediated photodynamic treatment (80 J/cm^2), Espitia-Almeida et al. [14] observed a 50% reduction in the viability of *L. panamensis* and *L. braziliensis* promastigotes when other Zn (II) porphyrin derivative at 1.2 and 11.6 μM, respectively, were applied. In that study, however, the authors used hydrophobic porphyrins and 24 h incubation time. Recently, Andrade et al. [17] applied

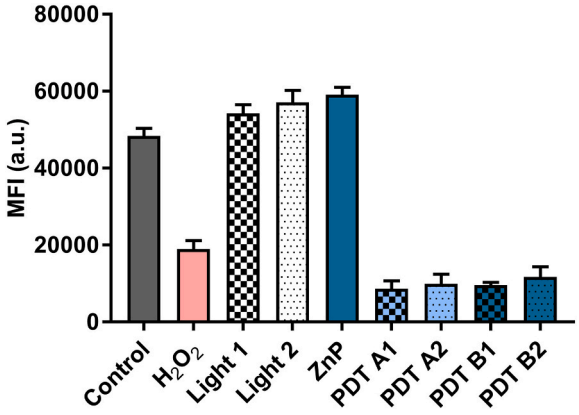

Fig. 3. Mitochondrial membrane potential for *L. amazonensis* promastigotes evaluated by flow cytometry using Rh 123. Median fluorescence intensity (MFI) of **Control –** untreated cells; **H_2O_2** (2.5%) **–** positive control for cell death; **ZnP –** 1.25 μM ZnP hexyl; **Light 1** (2.3 J/cm^2); **Light 2** (3.4 J/cm^2); **PDT A1 –** 0.62 μM ZnP hexyl + Light 1; **PDT A2 –** 0.62 μM ZnP hexyl + Light 2; **PDT B1 –** 1.25 μM ZnP hexyl + Light 1; **PDT B2 –** 1.25 μM ZnP hexyl + Light 2. Data presented as mean ± SE. For each sample, a total of 20,000 events were acquired and carried out in two independent assays.

photodynamic treatment (90 J/cm^2) mediated by hydrophilic ZnP ethyl (10 μM) and observed damages in *ca.* 90% of *L. braziliensis* promastigotes. Andrade and co-authors also found 50% of PI positive *L. braziliensis* promastigotes after the photodynamic treatment. Thus, it is worth noting that the lipophilic degree of the PS can influence the PDI performance on promastigotes. An increase in the aliphatic side-chain of the porphyrin confers a higher amphiphilic character to the PS, probably promoting greater interaction with the cell membrane, which may contribute to the increased efficiency observed by us for PDI mediated by ZnP hexyl. This pattern was observed for other cell types. For example, Moghnie et al. [15] also noted greater damage to the plasma membrane of *Saccharomyces cerevisiae* yeast cells after photodynamic treatment with ZnTnHex-2-PyP^{4+}, compared to more hydrophilic porphyrin analogues.

Thus, the experimental protocol mediated by ZnP hexyl was highly efficient for the photoinactivation of promastigotes of two *Leishmania* species. It led to a drastic reduction in cell viability, applying a lower radiant exposure, shorter pre-incubation time (5 min), and lower PS concentration, compared with studies that used other porphyrin derivatives, or even different families of PSs, such as chlorin e6, curcumin, and methylene blue (MB) [5,9,10,14,17,43,44].

3.3. Mitochondrial membrane potential (ΔΨm) evaluation

Rhodamine 123 (Rh 123) is a fluorescent dye that can be used to monitor the potential of the mitochondrial membrane. A decrease in Rh 123 fluorescence intensity indicates depolarization of the mitochondrial membrane, while an increase indicates hyperpolarization [40]. All samples of promastigotes photodynamically treated with ZnP hexyl showed relevant mitochondrial potential changes, different from cells treated only with light and the PS in the dark, according to flow cytometry analysis (Fig. 3).

In photodynamically treated samples, medians of fluorescence intensity (MFIs) decreased sharply (Fig. 3), indicating depolarization of the parasite mitochondrial membrane. As expected, the treatment with positive control (H_2O_2 – 2.5%) also led to accentuated ΔΨm depolarization. The Rh 123 results indicate that there were changes in ΔΨm, and consequently, damage to the parasite mitochondrion induced by the photodynamic treatment. Mitochondrial potential results for *L. braziliensis* followed a similar behavior to *L. amazonensis* and are presented in the Supplementary Material – Section E Fig. S4.

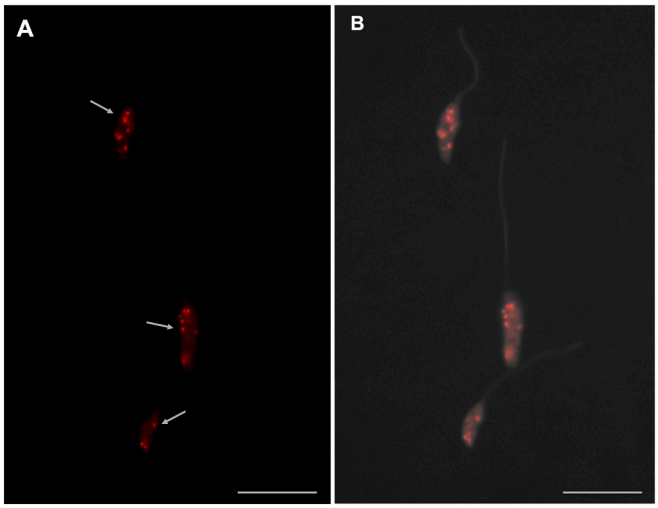

Fig. 4. Confocal fluorescence microscopy images of *L. amazonensis* promastigotes. **A –** Labeling of promastigotes by ZnP hexyl (5 μM), after 15 min of incubation (in red). **B –** The parameters were enhanced to reveal the autofluorescence of cells in gray. A punctate labeling pattern is observed along with the parasite cytoplasm. Scale bar: 10 μm.

The decrease in Rh 123 MFIs suggests an increase in the proton permeability across the internal mitochondrial membrane, resulting in a partial reduction, or complete inhibition, of ATP synthesis and, consequently, the death of the parasite. This is critical for protozoa of the *Leishmania* species, which have a single mitochondrion and are not able to properly compensate for any damage in this organelle, as opposed to mitochondrial damages occurring in mammalian cells. Thus, the parasite survival requires the correct performance of the mitochondrial respiratory chain [45].

The intense mitochondrial membrane depolarization noted in our study after the photodynamic treatment mediated by ZnP hexyl was the opposite of ΔΨm reported by Andrade et al. [17] for ZnP ethyl. They observed a noteworthy mitochondrial membrane hyperpolarization in samples photodynamically treated with ZnP ethyl. Andrade and co-authors [17] ascribed their result to a final attempt of the cells to prevent death since mitochondrial depolarization could be preceded by a high transient hyperpolarization.

Therefore, the distinct ΔΨm behavior followed by PDI with ZnP hexyl strengthens our viability results, indicating an enhanced interaction with the cell membrane, which is consistent with a greater intracellular PS bioavailability, impacting the mitochondrion, and leading to an effective cell death.

The closely related Mn(III) porphyrin analogs, MnP ethyl and MnP hexyl, also exhibited a different subcellular affinity [46,47]. The increase in the alkyl side chain was associated with an increase in the mitochondrial-to-cytosol ratio when Mn(III) porphyrin analogs were employed [48]. In a yeast model, the mitochondria-to-cytosol ratio for MnP ethyl was about 2, whereas this ratio was >10 for the more lipophilic MnP hexyl compound, *i.e.*, the concentration of MnP hexyl was 10-fold higher in the mitochondria than in the cytosol [49]. Studies with Zn(II) porphyrin analogues have also pointed out a high affinity of ZnP hexyl for mitochondria of cancer cells [12,20]. Overall, the subcellular localization of Zn(II) complexes based on *N*-alkylpyridylporphyrins mimic the behavior of their MnP counterparts: the increase in the length of the pyridyl alkyl chains affects the bulkiness/planarity of the molecule, directing the distribution of ZnPs from predominantly lysosomal (shorter alkyl chains, such as ZnP ethyl) to mitochondrial sites (longer alkyl chains, such as ZnP hexyl) [50].

Thus, the intracellular distribution pattern reported for ZnPs and related MnPs in different cell models may support the results found in the ΔΨm for promastigotes forms of *Leishmania* after photodynamic

treatment with ZnP hexyl.

3.4. Promastigote labeling by ZnP hexyl

ZnP hexyl *per se* presents a strong fluorescence, so this property was exploited to trace its intracellular fate in promastigotes of *L. amazonensis,* as shown in Fig. 4.

Our results revealed that parasites incubated with ZnP hexyl efficiently uptake this PS. The labeling showed that ZnP hexyl is distributed along with the parasite cytoplasm. We believe that this labeling shows a pattern similar to that observed in studies using mitochondrial-specific dye, such as MitoTracker [51,52]. Thus, based on Fig. 4 and the promastigote cell morphology, we hypothesize that the ZnP hexyl may accumulate in the mitochondrion or in other well-defined structures close to it. It is well known that the action of ROS is more effective in sites where the PS interacts. The PS needs to be close to biomolecules, such as lipids, to efficiently oxidize them [53]. Thus, we also believe that the photodynamic effect on the mitochondrial membrane potential, described in the previous section, also suggests an interaction of ZnP hexyl with the mitochondrion.

Since there was no difference in the labeling profile after 5 or 15 min of PS-cell interaction, this also suggests that the pre-incubation time, adopted in the photodynamic assays, was sufficient to an effective PS uptake by the parasites. No fluorescence was observed in flagellum.

An efficient PS uptake and its cellular location is relevant for a successful PDI. Herein, promastigotes also incubated with ZnP ethyl under the same conditions as applied to ZnP hexyl, showed no cell labeling by ZnP ethyl (data not shown). We believe that this difference between these porphyrins may be attributed to the higher lipophilicity of ZnP hexyl, enhancing its interaction with cell membrane and promoting greater intracellular bioavailability. High retention of ZnP hexyl by cancer cells was also observed by Benov and co-authors [19], with lower concentrations than ZnP ethyl.

Therefore, we demonstrated that ZnP hexyl was promptly interiorized by promastigotes and a punctate labeling could be observed into parasites after 5 min of incubation with this PS.

3.5. Morphological analysis of promastigotes

The morphological analysis by SEM showed that control *L. amazonensis* promastigotes (untreated) and Light 2 groups maintained their morphological characteristics, showing an elongated and fusiform body, with well-preserved smooth membrane and a single flagellum (Fig. 5A and B). Cells treated only with 1.25 μM ZnP hexyl in the dark did not show detectable changes in their morphology (Fig. 5C).

In contrast, parasites submitted to photodynamic treatment showed morphological alterations, such as increased cell volume and wrinkled plasma membrane, which are suggestive of change in the osmotic equilibrium and alteration in membrane permeability (Fig. 5D and E). Those observations corroborate the results of PI and trypan blue assays.

Changes in the parasite membrane are likely explained by the oxidation of proteins and lipids promoted by ROS formation. The presence of oxidized lipids, for example, can affect the biophysical properties of the membrane, such as its permeability and organization [54].

SEM characterizations of *L. braziliensis* promastigotes photodynamically treated with ZnP ethyl, reported by Andrade and co-authors, also indicated morphological changes like those observed above for *L. amazonensis* [17]. Akilov et al. and other authors [43,44,55], using different classes of PSs, also observed changes similar to those reported in the present study in *Leishmania* promastigotes using light microscopy. The authors also reported modifications of the elongated and fusiform body of the parasite, resulting in a round shape. Such modifications in the cell body may also occur due to the loss of cytoskeleton integrity [56].

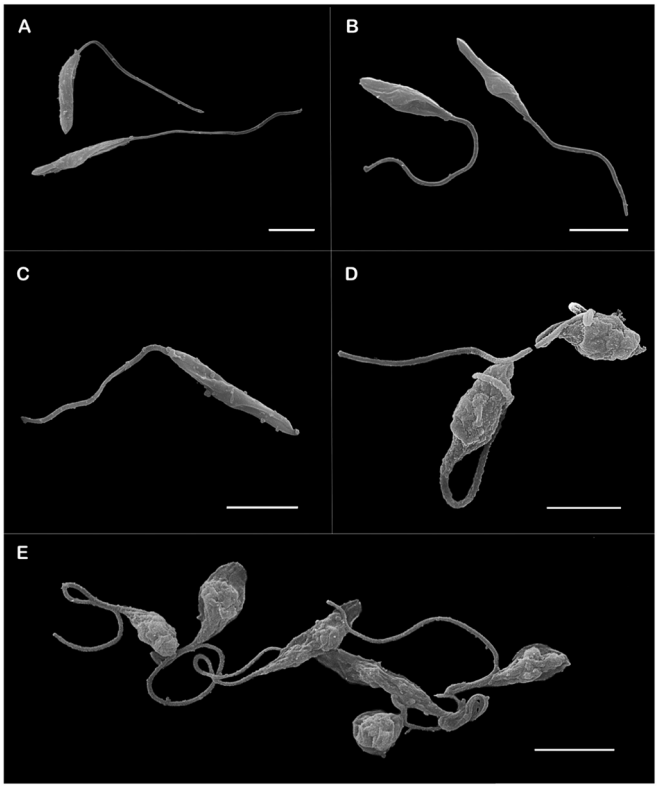

Fig. 5. *L. amazonensis* promastigotes observed by scanning electron microscopy. **A –** Control (without treatment); **B –** Light 2 (3.4 J/cm^2); **C –** 1.25 μM ZnP hexyl; **D –** 1.25 μM ZnP hexyl + Light 2 (PDT B2); **E –** 0.62 μM ZnP hexyl + Light 2 (PDT A2). Scale bar: 5 μm.

3.6. Cytotoxicity on mammalian cells

Cytotoxicity assays were performed with macrophages applying the higher radiant exposure (PDT A2 and PDT B2). Cells treated only with 1.25 μM ZnP in the dark did not show changes in the macrophage viability (Fig. 6). Samples irradiated only with light (Light 2) presented an increased response compared to the control. It is already known that blue light irradiation can exert regulatory effects on mitochondrial activity, proliferation, and differentiation of certain mammalian cell types

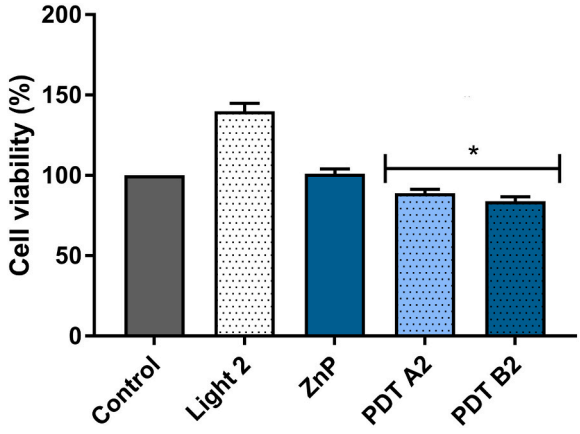

Fig. 6. Macrophage viability evaluated by MTT assay. **Control –** untreated cells; **Light 2 –** 3.4 J/ cm^2; **ZnP –** 1.25 μM ZnP hexyl; **PDT A2 –** 0.62 μM ZnP hexyl + Light 2; **PDT B2 –** 1.25 μM ZnP hexyl + Light 2. Data presented as mean ± SE. * Statistically significant groups ($p < 0.05$) when compared to control. Tests were performed in triplicates in three independent experiments ($n = 9$).

[57,58].

It is also worth mentioning that, although primary cultures are in general more sensitive when compared to immortalized macrophage lineages [59], the samples photodynamically treated with ZnP hexyl (0.62 or 1.25 μM) showed viability greater than 80%. There were no noteworthy differences between the photodynamic treatments with ZnP hexyl in all the concentrations tested.

The differences observed after photodynamic treatment, between the viabilities of promastigotes and macrophages, may be attributed to the higher sensitivity of the parasites towards oxidative stress, as previously suggested by other authors [8,60–62]. The antioxidant defense of trypanosomatids is based on the trypanothione reductase system, which has a rudimentary and deficient response against oxidative stress induced by drugs or photodynamic treatment [62,63]. The enzymes catalase and selenocysteine-containing glutathione peroxidases, present in mammals, are absent in these parasites. Besides, classical glutathione peroxidase in mammals reacts 10–100-fold faster than the tryparedoxin peroxidase, one of the enzymes of the trypanothione reductase system [60]. Different from mammalian cells, *Leishmania* cells have only a single mitochondrion. Thus, damage induced by ROS generation on the unique mitochondrion of these protozoans tends to be more severe [45].

Additionally, the PS concentration and light parameters employed can be a limiting factor for photocytotoxicity in mammalian cells [15]. For example, the viability after photodynamic treatment (3.4 J/cm^2) with 5 μM ZnP hexyl was lower, nearly 60% (data not shown), than for 0.65 and 1.25 μM (Fig. 6).

Andrade et al. [17], using 10 μM ZnP ethyl and a radiant exposure of 90 J/cm^2, observed a decrease of *ca.* 50% in BALB/c mouse peritoneal macrophages obtained from primary culture. Unlike our result, studies on other classes of PS, such as Bengal Rose dye derivatives, for example, showed that this compound, although presenting a high level of leishmanicidal activity, was toxic to J774 macrophages, even in the dark [64].

Thus, the results of cytotoxicity herein obtained suggest that ZnP hexyl is a promising PS and should be evaluated in *in vivo* CL studies. Furthermore, the localized treatment provided by PDI, associated with lower concentrations of PS and minor irradiation conditions, may also help to modulate and control the photodamage extension [65].

Table 1
Photodynamic effect of ZnP hexyl on the number of *L. amazonensis* intracellular amastigotes/macrophage, % of infection, and infection index. The infection index was calculated following the equation: number of amastigotes/macrophage × percentage of infection. These parameters were evaluated under light microscopy in samples stained with panoptic. **Control –** untreated cells; **PDT A2 –** 0.62 μM ZnP hexyl + Light 2; **PDT B2 –** 1.25 μM ZnP hexyl + Light 2. Light 2 – 3.4 J/cm^2. Results expressed as mean ± SE. *Statistically significant groups ($p < 0.05$) when compared to control. This evaluation was performed in duplicate, in three independent assays, totaling 600 cells analyzed ($n = 6$).

Groups	Intracellular amastigotes per macrophage	% Infection	Infection Index
Control	6.5 ± 0.8	90 ± 0.7	579.5 ± 77.6
PDT A2	3.0 ± 0.6*	75 ± 4.5*	244.5 ± 68.8*
PDT B2	2.3 ± 0.5*	70 ± 5.4*	176.1 ± 50.2*

3.7. Photodynamic effect on amastigotes

The infection resulted in an average number of 6.5 amastigotes per macrophage, with an infection rate of 90%. Table 1 presents the photodynamic effect associated with ZnP hexyl on peritoneal macrophages infected with *L. amazonensis*, at the highest radiant exposure (PDT A2 and PDT B2).

There were no significant differences among the Control, ZnP, and Light 2 groups for any parameter presented. On the other hand, the photodynamic treatment mediated by ZnP hexyl, reduced the number of amastigotes/macrophage by about 54% at 0.62 μM, and close by 64% at 1.25 μM. Furthermore, the infection index decreased approximately by 58% for PDT A2 and by 70% for PDT B2, after a single treatment session.

Also quantifying the number of intracellular amastigotes under light microscopy, Oliveira et al. [66] showed a similar reduction in the infection index (71%) using MB (another class of PS) to mediate PDI of *L. braziliensis*, but applying a PS concentration more than 30-fold higher than the one used in this present study. Likewise, in the PDI study of Andrade et al. with ZnP ethyl [17], a reduction of 40% in the number of amastigotes infecting macrophages *in vitro* was reported, also using a higher concentration (10 μM) than we employed. Therefore, our set of results highlights the potential of ZnP hexyl-mediated PDI for CL.

Fig. 7 shows two representative microscope fields illustrating the reduction in the number of intracellular amastigotes, at light microscope resolution, after photodynamic treatment session with 0.62 μM ZnP hexyl (Fig. 7B), compared to untreated cells (Fig. 7A). Fewer infected macrophages can be observed in Fig. 7B.

Thus, the data obtained herein indicated a great potential for ZnP hexyl as PS, suggesting that this Zn(II) porphyrin is a strong candidate for evaluation in *in vivo* studies.

4. Conclusion

The photodynamic treatment of *Leishmania* parasites mediated by ZnTnHex-2-PyP^{4+} showed efficiency *in vitro* using a submicromolar concentration of PS, with short pre-incubation and irradiation times, stimulating the evaluation of this Zn(II) porphyrin in pre-clinical assays. Our results also encourage further studies focused on investigation of the action and effects involved in the antimicrobial PDI mediated by Zn(II) porphyrins.

Author contributions

T.H.S.S. executed the study and collected data; C.G.A., F.V.C., and J.

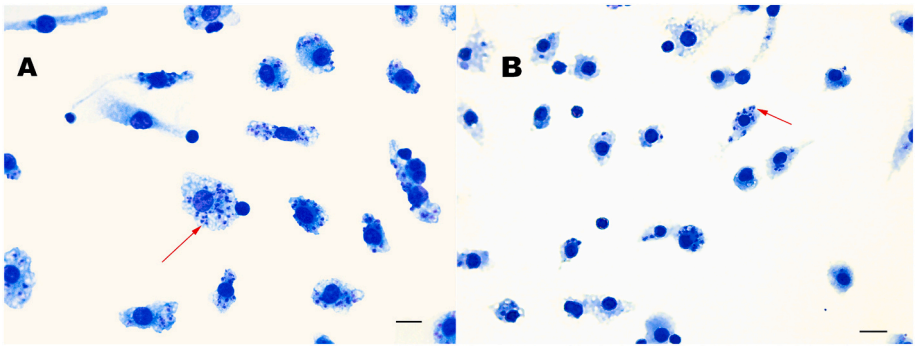

Fig. 7. Representative light microscopy images of infected macrophages stained with panoptic. **A –** Untreated (control), and **B –** after photodynamic treatment (PDT A2 – 0.62 μM ZnP hexyl + Light 2). Light 2 – 3.4 J/cm^2. Scale bar: 10 μm. Red arrows indicate intracellular amastigotes in the infected cells.

F.S.N. contributed to the data acquisition; J.F.S.N. and J.S.R. prepared and characterized the ZnP hexyl; J.S.R., B.S.S., M.S.R., R.C.B.Q.F., and A.F. were involved in the experimental design, and analyzed and discussed the results. All authors revised and approved the manuscript.

Credit author statement

T.H.S.S. executed the study and collected data; C.G.A., F.V.C., and J. F.S.N. contributed to the data acquisition; J.F.S.N. and J.S.R. prepared and characterized the ZnP hexyl; J.S.R., B.S.S., M.S.R., R.C.B.Q.F., and A.F. were involved in the experimental design, and analyzed and discussed the results. All authors revised and approved the manuscript.

Declaration of Competing Interest

The authors declare no competing interests.

Acknowledgments

We are grateful to the Núcleo de Plataformas Tecnológicas of the Instituto Aggeu Magalhães – Fundação Oswaldo Cruz (IAM/FIOCRUZ), Financiadora de Estudos e Projetos (FINEP), Conselho Nacional de Desenvolvimento Científico e Tecnológico (CNPq), Coordenação de Aperfeiçoamento de Pessoal de Nível Superior (CAPES), Centro de Apoio à Pesquisa (CENAPESQ - UFRPE), Fundação de Amparo à Ciência e Tecnologia de Pernambuco (FACEPE), and Fundação de Amparo à Pesquisa do Estado de São Paulo (FAPESP). This study is also associated with the Instituto Nacional de Ciência e Tecnologia em Fotônica (INFo). The English text of this paper has been revised by Sidney Pratt, Canadian, MAT (The Johns Hopkins University), RSAdip - TESL (Cambridge University).

Appendix A. Supplementary data

Supplementary data to this article can be found online at https://doi.org/10.1016/j.bbagen.2021.129897.

References

[1] WHO, Leishmaniasis *(accessed on December 2019)*, https://www.who.int/news-room/fact-sheets/detail/l, 2019.
[2] S. Burza, S.L. Croft, M. Boelaert, Leishmaniasis, Lancet 392 (2018) 951–970.
[3] H. Goto, J.A.L. Lindoso, Current diagnosis and treatment of cutaneous and mucocutaneous leishmaniasis, Expert Rev. Anti-Infect. Ther. 8 (2010) 419–433.
[4] M.B. Johansen, G.B.E. Jemec, S. Fabricius, Effective treatment with photodynamic therapy of cutaneous leishmaniasis: a case report, Dermatol. Ther. 32 (2019), e13022.
[5] D. Song, et al., Photodynamic therapy using methylene blue to treat cutaneous Leishmaniasis, Photomed. Laser Surg. 29 (2011) 711–715.
[6] M.R. Hamblin, Antimicrobial photodynamic inactivation: a bright new technique to kill resistant microbes, Curr. Opin. Microbiol. 33 (2016) 67–73.
[7] N. Kashef, M.R. Hamblin, Can microbial cells develop resistance to oxidative stress in antimicrobial photodynamic inactivation? Drug Resist. Updat. 31 (2017) 31–42.
[8] C.D. Enk, Treatment of cutaneous Leishmaniasis with photodynamic therapy, Arch. Dermatol. 139 (2003) 432.
[9] J.G. Pinto, et al., In vitro evaluation of photodynamic therapy using curcumin on Leishmania major and Leishmania braziliensis, Lasers Med. Sci. 31 (2016) 883–890.
[10] F.V. Cabral, et al., Preclinical investigation of methylene blue-mediated antimicrobial photodynamic therapy on Leishmania parasites using real-time bioluminescence, Photochem. Photobiol. 3 (2019) 604–610.
[11] J. Soriano, et al., Cell death mechanisms in tumoral and non-tumoral human cell lines triggered by photodynamic treatments: apoptosis, necrosis and parthanatos, Sci. Rep. 7 (2017) 41340.
[12] R. Ezzeddine, et al., Effect of molecular characteristics on cellular uptake, subcellular localization, and phototoxicity of Zn(II) N -alkylpyridylporphyrins, J. Biol. Chem. 288 (2013) 36579–36588.
[13] C. Pavani, Y. Iamamoto, M.S. Baptista, Mechanism and efficiency of cell death of type II photosensitizers: effect of zinc chelation†, Photochem. Photobiol. 88 (2012) 774–781.
[14] F. Espitia-Almeida, C. Díaz-Uribe, W. Vallejo, D. Gómez-Camargo, A.R. Romero Bohórquez, In vitro anti-leishmanial effect of metallic meso-substituted porphyrin derivatives against leishmania braziliensis and leishmania panamensis promastigotes properties, Molecules 25 (2020) 1887.
[15] S. Moghnie, A. Tovmasyan, J. Craik, I. Batinic-Haberle, L. Benov, Cationic amphiphilic Zn-porphyrin with high antifungal photodynamic potency, Photochem. Photobiol. Sci. 16 (2017) 1709–1716.
[16] K. Alenezi, A. Tovmasyan, I. Batinic-Haberle, L.T. Benov, Optimizing Zn porphyrin-based photosensitizers for efficient antibacterial photodynamic therapy, Photodiagn. Photodyn. Ther. 17 (2017) 154–159.
[17] C.G. Andrade, et al., Photodynamic effect of zinc porphyrin on the promastigote and amastigote forms of Leishmania braziliensis, Photochem. Photobiol. Sci. 17 (2018) 482–490.
[18] R. Al-Mutairi, A. Tovmasyan, I. Batinic-Haberle, L. Benov, Sublethal photodynamic treatment does not lead to development of resistance, Front. Microbiol. 9 (2018) 1699.
[19] L. Benov, J. Craik, I. Batinic-Haberle, The potential of Zn(II) N-alkylpyridylporphyrins for anticancer therapy, Anti Cancer Agents Med. Chem. 11 (2011) 233–241.
[20] A.M. Odeh, et al., Targeting mitochondria by Zn(II)N-alkylpyridylporphyrins: the impact of compound sub-mitochondrial partition on cell respiration and overall photodynamic efficacy, PLoS One 9 (2014), e108238.
[21] O. Viana, et al., Comparative study on the efficiency of the photodynamic inactivation of Candida albicans using CdTe quantum dots, Zn(II) porphyrin and their conjugates as photosensitizers, Molecules 20 (2015) 8893–8912.
[22] M. Minekus, et al., A standardised static in vitro digestion method suitable for food – an international consensus, Food Funct. 5 (2014) 1113–1124.
[23] P. Hambright, B. Shears, B. Shad, Acid-catalyzed solvolysis reactions of zinc porphyrins having various basicities and zinc N-methylporphyrins, J. Am. Chem. Soc. 93 (1971) 776–778.
[24] K.A. Connors, Chemical Kinetics: The Study of Reaction Rates in Solution, VCH Publishers Inc, 1990, pp. 34–39.
[25] L. Benov, I. Batinić-Haberle, I. Spasojević, I. Fridovich, Isomeric N-alkylpyridylporphyrins and their Zn(II) complexes: inactive as SOD mimics but powerful photosensitizers, Arch. Biochem. Biophys. 402 (2002) 159–165.
[26] W. Strober, Trypan blue exclusion test of cell viability, in: Current Protocols in Immunology, John Wiley & Sons, Inc, 2001.
[27] A. Aliança, et al., The in vitro biological activity of the Brazilian Brown seaweed Dictyota mertensii against Leishmania amazonensis, Molecules 19 (2014) 14052–14065.
[28] H. Sies, Findings in redox biology: from H 2 O 2 to oxidative stress, J. Biol. Chem. 295 (2020) 13458–13473.
[29] F.V. Cabral, et al., Nitric oxide-loaded chitosan nanoparticles as an innovative antileishmanial platform, Nitric Oxide 93 (2019) 25–33.
[30] P. Hambright, The chemistry of water-soluble porphyrins, in: K. Kadish, K. M. Smith, R. Guilard (Eds.), The Porphyrin Handbook, Elsevier, 2000, pp. 129–208.
[31] M. Inamo, et al., Equilibria, kinetics and mechanism of complexation of 5,10,15,20-tetrakis(4-sulfonatophenyl)porphyrin and its N-methylated derivative with cadmium(II) and zinc(II) ions in aqueous solution at various temperatures and pressures, Effects of metal ion size a, Inorg. Chim. Acta 256 (1997) 77–85.
[32] P. Hambright, P.B. Chock, Metal-porphyrin interactions, III. A dissociative interchange mechanism for metal ion incorporation into porphyrin molecules, J. Am. Chem. Soc. 96 (1974) 3123–3131.
[33] J. Nwaeme, H. Peter, Magnitudes of ionic strength effects in porphyrin metalation and acid solvolysis reactions, J. Inorg. Chem. 23 (1984) 1990–1992.
[34] Brasil, Resolução - RDC Nº 318, DE 6 DE NOVEMBRO DE 2019, *Ministério da Saúde Agência Nacional de Vigilância Sanitária*, 2019, p. 97. http://www.in.gov.br/web/dou/-/resolucao-rdc-n-318-de-6-de-novembro-de-2019-226513805.
[35] P. Hambright, T. Gore, M. Burton, Synthesis and characterization of new isomeric water-soluble porphyrins. Tetra (2-N-methylpyridyl) porphine and tetra (3-N-methylpyridyl) porphine. *J*, Inorg. Chem. 15 (1976) 2314–2315.
[36] J. Davila, A. Harriman, M.-C. Richoux, L.R. Milgrom, Sterically-hindered zinc porphyrins for solar-energy conversion, J. Chem. Soc. Chem. Commun. 7 (1987) 525–527.
[37] P. Hambright, I. Batinić-Haberle, I. Spasojević, Meso tetrakis ortho-, meta-, and para- N -alkylpyridiniopor-phyrins: kinetics of copper(II) and zinc(II) incorporation and zinc porphyrin demetalation, J. Porphyrins Phthalocyanines 07 (2003) 139–146.
[38] B. Shah, P. Hambright, Acid catalyzed solvolysis reactions of zinc porphyrins, J. Inorg. Nucl. Chem. 32 (1970) 3420–3422.
[39] R.R. Allison, et al., Photosensitizers in clinical PDT, Photodiagn. Photodyn. Ther. 1 (2004) 27–42.
[40] D.B. Scariot, et al., Induction of early autophagic process on Leishmania amazonensis by synergistic effect of miltefosine and innovative semi-synthetic thiosemicarbazone, Front. Microbiol. 8 (2017) 255.
[41] R.C. Zauli-Nascimento, et al., In vitro sensitivity of Leishmania (Viannia) braziliensis and Leishmania (Leishmania) amazonensis Brazilian isolates to meglumine antimoniate and amphotericin B, Tropical Med. Int. Health 15 (2010) 68–76.
[42] E.P. de Silva, J. Mittmann, V.T.P. Ferreira, M.A.G. Cardoso, M. Beltrame, Photodynamic effects of zinc phthalocyanines on intracellular amastigotes of Leishmania amazonensis and Leishmania braziliensis, Lasers Med. Sci. 30 (2015) 347–354.
[43] J.G. Pinto, et al., Chlorin E6 phototoxicity in *L. major* and *L. braziliensis* promastigotes—In vitro study, Photodiagn. Photodyn. Ther. 15 (2016) 19–24.
[44] J.G. Pinto, et al., Evaluation of methylene blue as photosensitizer in promastigotes of Leishmania major and Leishmania braziliensis, Photodiagn. Photodyn. Ther. 18 (2017) 325–330.

[45] F.P. Garcia, et al., A3K2A3-induced apoptotic cell death of Leishmania amazonensis occurs through caspase- and ATP-dependent mitochondrial dysfunction, Apoptosis 22 (2017) 57–71.
[46] I. Batinić-Haberle, J.S. Rebouças, L. Benov, I. Spasojević, Chemistry, biology and medical effects of water-soluble metalloporphyrins, in: K. Kadish, K.M. Smith, R. Guilard (Eds.), Handbook of Porphyrin Science, World Scientific, 2011, pp. 291–393.
[47] J.B. Aitken, et al., Intracellular targeting and pharmacological activity of the superoxide dismutase mimics MnTE-2-PyP 5+ and MnTnHex-2-PyP 5+ regulated by their porphyrin ring substituents, Inorg. Chem. 52 (2013) 4121–4123.
[48] I. Spasojevic, et al., Bioavailability of metalloporphyrin-based SOD mimics is greatly influenced by a single charge residing on a Mn site, Free Radic. Res. 45 (2011) 188–200.
[49] A. Tovmasyan, J.S. Reboucas, L. Benov, Simple biological systems for assessing the activity of superoxide dismutase mimics, Antioxid. Redox Signal. 20 (2014) 2416–2436.
[50] I. Batinic-Haberle, et al., H2O2-driven anticancer activity of Mn porphyrins and the underlying molecular pathways, Oxidative Med. Cell. Longev. 2021 (2021) 1–23.
[51] D. Arnoult, et al., On the evolution of programmed cell death: apoptosis of the unicellular eukaryote Leishmania major involves cysteine proteinase activation and mitochondrion permeabilization, Cell Death Differ. 9 (2002) 65–81.
[52] C.A. Antwi, C.M. Amisigo, J.P. Adjimani, T.M. Gwira, In vitro activity and mode of action of phenolic compounds on Leishmania donovani, PLoS Negl. Trop. Dis. 13 (2019), e0007206.
[53] S. Kwiatkowski, et al., Photodynamic therapy – mechanisms, photosensitizers and combinations, Biomed. Pharmacother. 106 (2018) 1098–1107.
[54] T.F. Schmidt, L. Caseli, O.N. Oliveira, R. Itri, Binding of methylene blue onto Langmuir monolayers representing cell membranes may explain its efficiency as photosensitizer in photodynamic therapy, Langmuir 31 (2015) 4205–4212.
[55] O.E. Akilov, et al., The role of photosensitizer molecular charge and structure on the efficacy of photodynamic therapy against Leishmania parasites, Chem. Biol. 13 (2006) 839–847.
[56] A. Jiménez-Ruiz, et al., Apoptotic markers in protozoan parasites, Parasit. Vectors 3 (2010) 104.
[57] C. Opländer, et al., Effects of blue light irradiation on human dermal fibroblasts, J. Photochem. Photobiol. B Biol. 103 (2011) 118–125.
[58] S. Bakalian, et al., The effect of blue light exposure on the proliferation rate of human retinoblastoma cell lines, Invest. Ophthalmol. Vis. Sci. 46 (2005) 4261.
[59] P. Bourdeau, et al., Short-Term Toxicity Tests for Non-Genotoxic Effects / edited by Philippe Bourdeau ... [et al.]; prepared by Scientific Group on Methodologies for the Safety Evaluation of Chemicals (SGOMSEC), Published on behalf of the Scientific Committee on, 1990.
[60] A. Schmidt, R. Krauth-Siegel, Enzymes of the trypanothione metabolism as targets for antitrypanosomal drug development, Curr. Top. Med. Chem. 2 (2002) 1239–1259.
[61] S. Dutta, D. Ray, B.K. Kolli, K.-P. Chang, Photodynamic sensitization of Leishmania amazonensis in both extracellular and intracellular stages with aluminum phthalocyanine chloride for photolysis in vitro, Antimicrob. Agents Chemother. 49 (2005) 4474–4484.
[62] J.F. Turrens, Oxidative stress and antioxidant defenses: a target for the treatment of diseases caused by parasitic protozoa, Mol. Asp. Med. 25 (2004) 211–220.
[63] P.R.T. Romão, et al., Glutathione and the redox control system trypanothione/trypanothione reductase are involved in the protection of Leishmania spp. against nitrosothiol-induced cytotoxicity, Braz. J. Med. Biol. Res. 39 (2006) 355–363.
[64] T.R. Navasconi, et al., Photodynamic therapy with bengal rose and derivatives against Leishmania amazonensis, J. Lasers Med. Sci. 8 (2017) 46–50.
[65] K. König, H. Meyer, H. Schneckenburger, A. Rück, The study of endogenous porphyrins in human skin and their potential for photodynamic therapy by laser induced fluorescence spectroscopy, Lasers Med. Sci. 8 (1993) 127–132.
[66] S. de Oliveira, et al., Leishmanicidal effect of antiparasitic photodynamic therapy—ApPDT on infected macrophages, Lasers Med. Sci. 32 (2017) 1959–1964.